MR Cygni Revisited

Albert P. Linnell[1]

Department of Physics and Astronomy

Michigan State University

and

Josef Kallrath

Sternwarte der Universitat Bonn

Received 1986 August 25;

[1]Guest Investigator, International Ultraviolet Explorer Satellite, which is sponsored by the National Aeronautics and Space Administration, by the Science Engineering and Research Council of the United Kingdom, and by the European Space Agency.

ABSTRACT

New analysis tools and additional unanalyzed observations justify a reanalysis of MR Cygni. The reanalyses applied successively more restrictive physical models, each with an optimization program. The final model assigned separate first- and second-order limb darkening coefficients, from model atmospheres, to individual grid points.

Proper operation of the optimization procedure has been tested on simulated observational data, produced by light synthesis with assigned system parameters, and modulated by simulated observational error. The iterative solution converged to a weakly-determined mass ratio of 0.75. The system has deep partial eclipses. The bolometric albedo of the secondary has a strong effect at the shoulders of secondary minimum. The iterative solution determined a value of $\underline{A}_2 = 0.53$. This result is in contrast to the theoretically expected value of 1.0. The same result follows with two independent light synthesis programs and with three independent sets of observational data.

Assuming the B3 primary component is on the main sequence, we calculate the HR diagram location of the secondary from the light ratio (ordinate) and adjusted T_{eff} (abscissa). To within the accuracy of these quantities, the secondary is a B7 main sequence object.

The derived mass ratio, $\underline{q}$, together with a main-sequence mass for the B3 component, implies a main-sequence secondary spectral type of B4. The photometrically-determined secondary radii agree with this spectral type, in marginal disagreement (3σ, estimated) with the B7 type from the HR diagram analysis.

The individual masses, derived from the radial velocity curve of the primary component, the photometrically-determined i, and alternative values of q are seriously discrepant with main sequence objects.

The imputed physical status of the system is in disagreement with representations that have appeared in the literature.

Subject headings: stars-atmospheres - stars: eclipsing binaries - stars: individual (MR Cyg)

I. Introduction

MR Cygni (BD+47°3639; SAO 051509) has been the subject of numerous light curve solutions. These have included Russell Model solutions by Lavrov (1965), Hall and Hardie (1969), Proctor and Linnell (1972), and Battistini, Bonifazi, and Guarniari (1972), Kopal method solutions by Söderhjelm (1974, 1978), and light synthesis solutions by Wilson and Devinney (1971, hereafter WD), Hill and Hutchings (1973a, hereafter HIH), and Eaton (1975). All of the solutions later than 1965 have used the U, B, V, observational data of Hall and Hardie (1969, hereafter HAH). Two separate sets of V, B observations have been published since 1969: Battistini, Bonifazi, and Guarnieri (1972, hereafter BBG) and Murnikova and Paramonova (1980, hereafter MP). The BBG data were included in the second analysis by Söderhjelm (1978); MP data have not been the subject of a light synthesis analysis.

Several additional considerations commend a new light synthesis study of this system. These considerations are the following: (1) The WD solution used an initial version of the WD light synthesis program. The initial separate wavelength solutions were superseded by a simultaneous B, V solution (Wilson and Devinney 1972, hereafter WDII). The original WD program was modified to effect an improved treatment of the reflection effect (Wilson, DeLuccia, Johnston, and Mango 1972). (See also the description of operating modes in Leung and Wilson (1977) and further description of differential corrections in Wilson (1979)). The WDII solution has the undesirable property of requiring negative limb darkening coefficients for the secondary component in both B and V. (2) There is substantial variation among the different light synthesis solutions of the same observational data. Thus, the Eaton and HIH solutions derived total

eclipses while the WD solution did not. (3) With the exception of Söderhjelm's study, none of the published light synthesis solutions provide residuals plots, We regard residuals plots as essential elements of any definitive solution. (4) The HIH and WD (and WDII) solutions used normal points. It is our contention that individual observations should be used rather than normal points. The power of widely available computers has improved to the point where individual observations now can easily be used. (5) Neither the HIH nor the two WD solutions included the mass ratio, q, as a variable parameter. Different choices for q, from spectroscopic sources, led to very different physical conditions. (6) The evolutionary state of the system, inferred from the derived system parameters, is very different in the various analyses. HAH obtain uncomplicated main sequence B3 and B8 components. WD and Eaton obtain an overluminous secondary which they suggest may still be contracting to the main sequence. HIH derive slightly evolved primary and secondary components, with the primary component nearing hydrogen core exhaustion. Söderhjelm argues for a semi-detached post mass-transfer object. (7) We have available a powerful new parameter optimization procedure (Kallrath and Linnell 1987, hereafter KL). (8) None of the prior optimization solutions provides an independent test of the solution convergence properties, described subsequently. We propose this test as an important element in light synthesis solutions. Specifically, we argue that synthetic "observational" data should be generated with known system parameters agreeing with the derived parameters for the actual observations of the system under study, the data should be modulated with simulated observational errors, and the resultant data should be analyzed with the same procedure used to discuss the actual observational data. It should be demonstrated that system parameters originally specified for the

synthetic data can be recovered to appropriate accuracy within the number of iterations actually applied, and that the final iteration represents a stable situation not subject to significant further change with additional iterations. The starting parameters for the analysis of the synthetic data should differ from the known parameters by at least as much as was true for the analysis of the actual data. This is not a new proposal. Linnell (1973), Hill (1979) and Popper (1984) have made similar proposals. It is not sufficient to test proper operation of the program, from a structural standpoint, by a number of initial analyses of this type. Rather, a simulation test of the type proposed should be performed for each system being analyzed. An iterative solution is a highly nonlinear process. Convergence properties are not global; they should be checked separately with each new parameter set.

Section II of this paper presents details of our MR Cyg solutions. Section III discusses the BBG data, and section IV, the MP data. Section V contains a discussion of the system physical status. Conclusions are in Section VI.

II. System Solution, HAH Data

We begin with a study of the HAH data. The original WD solution was done in mode 0, by separate wavelengths. Subsequent elaboration with additional modes provided more realistic physics, described by Leung and Wilson (1977). We started with the final system parameters from the WD solution and applied our simplex technique (KL) to the individual light curves, using the newer (1977) WD program in mode 2. One of us (JK) has further revised the WD program to run in double precision on our VAX computer. Optimization with the simplex algorithm is under control of a program called LCCTRL (Kallrath and Linnell 1987). Only that portion of the

WD differential corrections subroutine which generates a synthetic light curve actually is called by LCCTRL. Thus the optimization reported here for the WD program makes no use of the WD differential corrections procedure itself.

All of our solutions assigned weights to the individual observations proportional to $\ell^{1/2}$, where ℓ is the light value. We optimized on the individual observations. The results of that optimization, after 60 iterations, are in KL, Table 1. Briefly, we effected a substantial further reduction in the variance of the individual B, V light curves. A plot of the individual residuals from the WD mode 0 solution (using the newer version of the WD program) indicates the probability that the original solution had not converged completely. That plot appears in KL, Figure 8. The adopted polar temperature of the primary, 18000K, agreed with the WD study.

The separate U solution fits the observations well and produces system parameters in good agreement with the V, B solutions except for T_2, the polar temperature of the secondary.

A systematic trend is apparent (KL) at secondary minimum in the B and U residuals. No trend is apparent in the V residuals.

The separate simplex + WD program solutions produce positive limb darkening coefficients for the secondary component, an improvement over the original WD solution. However, the fractional luminosity of the primary changes in the wrong direction from V to B, but in the correct direction from B to U. This is the same difficulty in the original WD solution for B and V. The fact that the original WD solution was in mode 0, which leaves the fractional luminosities uncoupled to the polar temperatures, may have contributed to the unsatisfactory WD solution parameters. Both mode 0 and

mode 2, used in our separate V, B solutions, via the simplex algorithm, produced an improvement in the sense that the secondary component limb darkening coefficients no longer are anomalous. The simultaneous V, B solution in mode 2, described subsequently, produced fractional luminosities with the correct trend in wavelengths and also non-negative limb darkening coefficients.

The new light synthesis package, SYNPGM (Linnell 1984) assigns separate limb darkening coefficients to each photospheric grid point, determined from model atmospheres. Limb darkening should vary over the photosphere as local temperature and gravity vary. We place more faith in limb darkening coefficients from modern model atmospheres, in general, than in empirical values from typical light curve solutions. The control program LCCTRL, which implements the simplex algorithm, links either to WD or to SYNPGM to produce the theoretical light curves needed for comparison with observations. LCCTRL iterates to achieve a solution, as determined by appropriate criteria described in KL. Modern calibrations of effective temperature assign a temperature of 18700 to spectral class B3 (Schmidt-Kaler 1982, pp. 451 ff). Table 1 presents results of simultaneous B, V solutions, both with the WD program and SYNPGM. The WD solution used mode 0. We call attention to the increasing constraints in the physical models used by our successive analyses. The mode 0 solutions of the separate light curves represent the least constrained condition, and produce the smallest residuals, as expected. The simultaneous mode 2 solution exhibits slightly larger residuals. The SYNPGM solution is still more restrictive in that the limb darkening coefficient is no longer an adjustable parameter. Thus we expect a slightly larger standard deviation of residuals than with the simultaneous mode 2 WD solution. Figure 1 presents the light curve and V

residuals for the SYNPGM solution. The residuals for the B solution are in Figure 2. (Figure 7 shows the B fit.) As expected, the dispersion of residuals is slightly larger than for the individual light curve solutions. The previous systematic trend in the B residuals is no longer apparent. It is a curiosity that the B and V residuals appear to divide into two separate groups around primary minimum. There would be a reasonable suspicion that this indicates intrinsic variability of the star, or a problem with extinction corrections on different nights, except for the fact that no such effect is apparent on the individual wavelength solutions reported in KL. Figure 3 shows the U residuals, using the simultaneous solution parameters for the SYNPGM B and V solution. The calculated light curve is too shallow at primary minimum and too deep at secondary, indicating the need for a greater component temperature difference in U. We attribute this effect to failure of the black body approximation, since both light synthesis programs generate radiated flux at a given wavelength by use of the Planck law, together with the local effective temperature. We expect that a synthesized spectrum for the binary star, convolved with transmission of the earth's atmosphere and the U filter would improve the fit to the U data. Obvious uncertainty is involved because of different air masses for the separate observations, producing variable ultraviolet cutoff.

The initial SYNPGM fit, using the original WD parameters, produced appreciable residuals on the shoulders of secondary minimum, Figure 4 (B curve). The residuals arise almost entirely from the reflection effect. SYNPGM provides facilities to display the phase-wise light variation of each component separately, with eclipse effects removed. Figure 5 shows the light variation of the primary component. Note the slight departure of maximum light from phase quadrature. This arises from the nonsymmetrical

tidal distortion of the primary component, coupled with gravity brightening. Figure 6 shows the light variation of the secondary, assuming a bolometric albedo $\underline{A}_2 = 1.0$. The light variation is dominated by reradiation of light received from the primary. A reduction of $\underline{A}_2$ greatly improves the fit. Figure 7 shows the light curve fit in $\underline{B}$ with $\underline{A}_2 = 0.50$. Figure 8 illustrates the light variation of the secondary alone, with $\underline{A}_2 = 0.50$. We permitted LCCTRL to adjust $\underline{A}_2$ with both the WD program and SYNPGM. As Table 1 indicates, the best fit value is $\underline{A}_2 = 0.53$ for both programs. We did not adjust $\underline{A}_1$ since the reflection effect for the primary is negligible. We discuss this result in Section V.

The Table 1 WD + simplex solution includes calculated probable errors. These were produced with the WD program differential corrections facility, although we used the simplex algorithm for optimization.

We note that $\underline{q}$, $\underline{\Omega}_1$, and $\underline{\Omega}_2$ are interrelated. For stars of small to moderate distortion, the simultaneous optimization problem in $\underline{\Omega}_1$, $\underline{\Omega}_2$, and $\underline{q}$ is not precisely defined. By this we mean that the sensitivity of $\underline{r}$ to changes in $\underline{\Omega}_1$, $\underline{\Omega}_2$, or $\underline{q}$, over the surface, is not very great for systems of this type. The simplex algorithm found a variety of combinations of these three quantities that give nearly identical values of the variance. In addition, there is an appreciable variation of $\underline{i}$ with changes in $\underline{q}$ and the $\underline{\Omega}$'s. This is an expected result, especially for a partially eclipsing system. Nonetheless, the data do produce a weakly determined value of $\underline{q}$ at about 0.75. The calculated formal error in the WD + simplex solution (Table 1) is unrealistically small. Our experience with the simplex solution leads us to estimate an uncertainty in $\underline{q}$ of about ± 0.07. This estimate comes from study of the solution of our synthesized light curve, modulated with simulated observational error. We found that the calculated $\underline{q}$ value

wandered in the range 0.69-0.82 for a known original q of 0.78. The simplex solution of the observational data produced q values, during iteration, also in the range $0.69 \lesssim q \lesssim 0.82$. In a similar manner we have estimated uncertainties for the other parameters subject to optimization. These estimates appear in the last column of Table 1. They are in parentheses to distinguish them from the formal probable errors for the WD solution.

The simplex algorithm applies the Kolmogorov-Smirnov goodness-of-fit test to a residuals histogram as a test for normal distribution of residuals. The V, B, and U residuals, from the simultaneous solutions, all failed this test. Residuals plots show systematic trends, already discussed.

III. System Solution, BBG Data

We obtained a solution of the BBG B data (490 individual points) with the simplex algorithm and the SYNPGM package. After 22 iterations the system parameters were those listed in Table 2. The values of i and T_2 are in close agreement with the Table 1 values. The interdependence of q, Ω_1, and Ω_2 has been discussed, as it affects the possibility of unique determination of individual values. Note that the A_2 value is in close agreement with the Table 1 values. This demonstrates that the anomalous value is not an artifact of the HAH data. The standard deviation of the residuals is small enough to give considerable weight to this determination.

IV. System Solution, MP Data

We obtained simultaneous solutions of the MP data in V and B, using the simplex algorithm and the SYNPGM package. The MP residuals are much larger than the other two data sets. Some individual residuals are so large that they almost certainly are typographical errors in the printed data. We entered both the BBG and MP data into our computer with the aid of a

Kurzweil document reader and proofread the results. Results of a simultaneous B, V solution, after 13 iterations, are in Table 3. In spite of the larger standard deviation of residuals, the calculated parameters are in close agreement with the other solutions. The differences among the different solutions are appreciably larger than the calculated formal errors in the WD solution, but are well within our estimated uncertainties. The discrepancy may be a result of the non-gaussian distribution of residuals.

V. MR Cygni Physical Status

It is worth reemphasis that the inference of system properties from an optimized light synthesis solution occurs through the aegis of a specific physical model. Obvious physical effects exist which are not a part of existing Roche models and which may be of importance at the level of about 0.01 magnitude. Photospheric distortion from radiation pressure may affect components of early spectral type. The Roche model, which coincides with a polytrope of index 5, does not give a precise representation of tidal and rotational distortion for radiative atmospheres ($n \sim 3$) or convective atmospheres ($n \sim 3/2$). Although synchronous rotation is likely, we have no direct information on this subject. Rotational distortion of an $n = 3$ polytrope differs from that of an $n = 5$ polytrope. A single bolometric albedo is inappropriate for an entire distorted, irradiated star, as is a single limb darkening coefficient. The adopted model atmosphere limb darkening coefficients may not be appropriate for the illuminated component faces. The distribution of radiation with wavelength, for the irradiated component, will differ significantly, on the irradiated face, from that of a corresponding nonirradiated star (Rucinski 1970). If the physics were sufficiently tractable and calculation of these effects sufficiently simple, the appropriate modelling technique would be a self-consistent calculation

in which the parameters initially determined by empirical adjustment were replaced by a complete closed calculation. That stage is yet to be achieved. The point of using believable physics is illustrated by the example of the Russell Model. The Proctor and Linnell (1972) Russell Model MR Cyg solution of the HAH data produced residuals plots with as small values as those of the present study. The argument for preferring the present solution therefore does not derive from the quality of the fit to available observational data. Similarly, our preference for the SYNPGM solution to the WD solution arises from the model atmosphere results that limb darkening should vary over a distorted star whose local gravity and temperature also vary.

We now consider the derived bolometric albedo $A_2 = 0.53$. This is an accordant result from two independent light synthesis programs that treat limb darkening differently. The result therefore is not an artifact of the way limb darkening is treated. The same result follows from all three data sets. It therefore is not an artifact of a single data set. Our separate tests with simulated observational data, produced by light synthesis from assigned system parameters and modulated with simulated observational errors, show that the number and quality of the actual data are sufficient to determine $\underline{A}_2$ with good accuracy. Our literature search shows that adoption of $\underline{A}_2 = 1.0$ is a universal procedure for light curve solutions of stars with radiative envelopes. Comparable evidence for other early type stars therefore is lacking at present. As already discussed, it is conceivable that the adopted physical model differs from physical reality and that the anomalous $\underline{A}_2$ result is an indirect consequence.

The theoretical result $\underline{A}_2 = 1.0$ has been discussed in the literature (Napier, 1971; see also the review article by Vaz 1985, and Vaz and Nordlund

1985). Napier records two possible mechanisms which could modify the theoretical value: (1) Incident energy is absorbed, transmitted horizontally by circulation currents, and reemitted elsewhere (proposed by Hosokawa). (2) Radiation from the deep interior is partly dammed up by the reflection effect. As Napier shows, the first mechanism cannot operate in radiative envelopes. Circulation currents induced by incident radiation have been studied by the Tassouls (Tassoul and Tassoul 1982c). They find that radiation-induced circulation currents are much slower than previously believed, and that these currents occur in a very thin surficial flow directed away from the substellar point on the irradiated star. The cooling time of a thin layer at the stellar surface is so short compared with the time required for circulation currents to transport matter a detectable distance on the surface that escaping reemitted radiation must occur at essentially the same point as absorption took place. Circulation currents induced by rotational and tidal distortion have also been analyzed by the Tassouls (Tassoul and Tassoul 1982a,b,c, 1983). The temperature gradient in a radiative envelope is steep enough that the enthalpy contribution from irradiation must be negligible at appreciable depth. Therefore any proposed effect due to "transported" energy should be confined very close to the surface. By the same argument already presented, the cooling time of surface layers is too short for fluid flow to effect measureable energy transport.

Napier's second mechanism requires solution of the transfer equation in the presence of an external irradiating source. Rucinski (1970) has made a detailed study of this problem in a case sufficiently similar to the present one for his results to be approximately valid. Rucinski finds irradiation produces an appreciable effect on the wavelength distribution of the

emergent radiation. Monochromatic albedoes show appreciable variation, both with wavelength and angle of incidence of irradiation. However, the weighted combination, the bolometric albedo, is close to 1.0. There is a genuine discrepancy between theory and observation.

The theoretical result assumes a static radiative atmosphere with an incident radiation field. Although rapid rotation violates the assumption and produces circulation currents, the latter are too slow, ipso facto, to redistribute the incident radiation. However, a different effect may operate. The Tassouls find (1982a) that rotating early type stars generate instabilities that in turn produce layered turbulence. We suggest that this turbulence may behave sufficiently like convective equilibrium to produce the observed A_2. Note that the bolometric albedo appropriate to convective equilibrium is 0.5 (Rucinski 1969). Underhill and Fahey (1984) show that OB stars may be unstable against convection because the adiabatic gradient is reduced by second ionization of helium and radiation pressure. The temperature regime of the Underhill and Fahey study lies above that pertaining to the photosphere of MR Cyg.

With these points in mind, consider the system physical status as implied by the light curve solutions.

We first consider the location of the separate components on the HR diagram. Figure 9 shows the HR main sequence with M_V and M_B values (Schmidt-Kaler 1982, p. 17ff) vs. $(B-V)_o$ values (Schmidt-Kaler 1982, p. 14ff). Also shown are effective temperatures (Schmidt-Kaler 1982, p. 451ff). We place the primary component on the main sequence at spectral class B3, T_{eff} = 18700K. IUE spectra, to be reported separately, show a close fit over the range λ1200-λ3200 to the B3V standard 17 Vul. The spectrum of the hotter component dominates in the λ1200-λ3200 interval. The

SYNPGM simultaneous solution gives the V light ratio of the components as well as a calculated T_{eff} of the secondary component (pole). For each component, that component T_{eff} is given as the T_{eff} for the pole. The polar T_{eff} should be slightly higher, but the solution is fairly insensitive to the absolute temperature as long as the component temperature difference remains appropriate. The calculated location of the secondary appears as a *. The probable error for T_{eff} shows as a horizontal error bar. We do not have a good means to estimate the error in M_V. The same procedure with the B data produces the point marked Δ. B error bar has been omitted since it is comparable to that for V. To within the probable errors of the relevant parameters, both components lie on the main sequence, and the spectral type of the secondary is B7. The intrinsic width of the main sequence is several tenths of a magnitude.

In our simulation we adopted a main sequence mass of 7.6 $M_\odot$ for the primary, since SYNPGM uses photospheric potentials in cgs units. (The data in Table 1 are the Roche model equivalent.)

Figure 10 shows the main sequence relation between stellar mass and spectral type (Schmidt-Kaler 1982, p. 31). The B7(+) spectral type deduced from Figure 9 implies a main sequence mass of 4.2 $M_\odot$, at the location indicated, and a corresponding q = 0.55. The limiting values of the photometric q, 0.70 and 0.80, together with the adopted mass for the primary, produce corresponding secondary mass values. On the assumption the secondary is a main sequence object, the arrows labelled q = 0.70 and 0.80 mark limits for the secondary based on the photometric q. Thus there is a discrepancy with the weakly-determined q from the light curve solution.

The system geometry from our solutions is in Figure 11.

Our solution indicates deep partial eclipses. No independent information is available to specify the evolutionary state of the primary B3 component. The HIH radial velocity curve clearly shows that the larger, higher surface brightness, B3 component is the one eclipsed at primary minimum. Consequently the Söderhjelm (1978) argument for a semi-detached post mass-transfer object must be discarded. Figure 9, based on modern data, shows that the secondary component is on the main sequence if the primary is. This result does not support the WD and Eaton argument for an overluminous secondary still contracting to the main sequence. We find no evidence to support the HIH argument that both components lie above the main sequence, with the primary nearing hydrogen core exhaustion. We do not believe the Figure 10 results indicate a serious discrepancy. The low weight determination of $\underline{q}$ and its interdependence with $\underline{\Omega}_1$ and $\underline{\Omega}_2$ has already been noted.

There is a serious discrepancy with the amplitude of the radial velocity curve. The spectroscopic study of Hill and Hutchings (1973b) determined a velocity amplitude of the primary component $\underline{K}_1 = 120.8$ km s^{-1}. The distance of the center of the primary component to the system center of mass then follows from the condition of a circular orbit, the known $\underline{i}$, and the period. The value is $\underline{a}_1 = 0.2807 \times 10^{12}$ cm. An assumed $\underline{q}$ gives the separation of components, $\underline{a}$, and Kepler's third law gives the sum of masses. For $\underline{q} = 0.55$, $\underline{M}_1 = 4.53\ \underline{M}_\odot$, $\underline{M}_2 = 2.49\ \underline{M}_\odot$. For $\underline{q} = 0.75$, $\underline{M}_1 = 2.27\ \underline{M}_\odot$, $\underline{M}_2 = 1.71\ \underline{M}_\odot$. Figure 10 shows the discrepancy between these values and those assumed for the photometric solution.

The calculated radius of the secondary is discrepant if the secondary is a main sequence B7 star. Schmidt-Kaler (1982, p. 30) provides a calibration of main-sequence radius vs. spectral type. Our Figure 11

representation of the secondary follows from the photometric solution radii. A main-sequence B7 star has a radius of about 3.2 $\underline{R}_{\odot}$. If one adopts the photometric $\underline{q}$, then the photometrically-determined radius and the imputed B4 spectral type, from $\underline{q}$, are in agreement. It could be argued that the secondary component is a main sequence object, of spectral type about B4, and the primary is overluminous, indicating evolution away from the main sequence. But the calculated radius of the primary would then be discrepant. Further, the effective temperature of an evolved star of $\sim 5\underline{M}_{\odot}$ is always less than its ZAMS effective temperature (Iben 1967). The temperature difference between components cannot be changed by more than about $\pm$200K without producing easily detectable discrepancies in the depths of the minima.

The best we can say is that we have achieved good photometric solutions with two different light synthesis programs, both based on a similar (Roche) physical model. The HR diagram component locations initially can be understood as main sequence B3+B7 objects. The masses of the objects are in serious disagreement with results from the radial velocity curve. The secondary is a normal B4 star based on the photometric $\underline{q}$ and photometrically-determined radii, but this result is abnormal based on the photometrically-determined luminosity ratio and temperature difference. A cross-correlation radial velocity study has the potential to detect the secondary component and so resolve the uncertainty concerning $\underline{q}$. This would be especially valuable in the present instance in view of the partial eclipses. We believe the present paper demonstrates an advance in technique for photometric solution of eclipsing binary light curves. This capability will produce its best astronomical contribution in collaboration with

spectroscopists using modern cross-correlation techniques for independent determination of mass ratios.

VI. Conclusions

1. Using the WD program in mode 2, we obtain a simultaneous V, B solution of the HAH data with the simplex algorithm. The derived limb darkening coefficients show improved agreement with Kurucz atmospheres, compared with the original WD solutions. None of the limb darkening coefficients is negative.
2. A solution of the same data, using SYNPGM as the numerical model, and optimized by the simplex algorithm, gave an excellent fit to the data.
3. The HAH, BBG, and MP data produce a weakly-determined photometric mass ratio of 0.75 ± 0.07 (estimated error).
4. Both the WD and SYNPGM solutions determine a bolometric albedo of about 0.5 for the secondary component. This result is accordant for the HAH, BBG, and MP data. This result is in disagreement with the theoretical value of 1.0, appropriate to static atmospheres in radiative equilibrium. A possible resolution of the discrepancy is layered turbulence, predicted theoretically by the Tassouls to be induced in early type stars by rapid rotation. A less likely alternative is convection induced by depression of the adiabatic gradient as studied by Underhill and Fahey.
5. Assuming the primary B3 component lies on the main sequence, the calculated location of the secondary places it on the main sequence also, at a spectral type of B7. The calculated location follows from the light ratio for the ordinate and the polar temperature for the abscissa.

6. Assuming a main sequence mass of 7.6 $M_{\odot}$ for the primary, the derived mass ratio would imply a secondary of spectral type B4. The secondary radius from the photometric solution agrees with this spectral type. This result is in marginal disagreement with point 5, at the estimated 3σ level.

7. The radial velocity curve, together with the photometrically-determined i, circular orbits, and alternative choices for q, leads to masses seriously discrepant with assumed main sequence objects.

TABLE 1

Simultaneous B, V solution with WD and SYNPGM programs.

Parameter	Wilson/Devinney 1972 BV,B(V)		Wilson+SIMPLEX BV[mode 2], B(V)		SYNPGM + SIMPLE B & V curve
i	82°89	± 0°23	83°03	± 0°03	82°50(±0°86)
L1	...	...	9.3610(9.2988)	±0.0236(0.0327)	1830 $L_\odot$
L2	...	...	2.8215(3.2352)	± 0.0071(0.0114)	340 $L_\odot$
ℓ1	0.7950(0.7785)	± 0.0059 (0.0059)	0.7684(0.7419)	± 0.0019(0.0026)	0.8431
ℓ2	0.2050(0.2215)	± 0.0054 (0.0055)	0.2316(0.2581)	± 0.0006(0.0009)	0.1569
x1	0.70 (0.65)	± 0.03 (0.04)	0.52 (0.59)	± 0.15 (0.02)	grid values
x2	0.00 (0.00)	± 0.00 (0.00)	0.14 (0.27)	± 0.18 (0.02)	adopted from Kurucz atmos
g1	1.00[a]		1.00[a]		1.00[a]
g2	1.00[a]		1.00[a]		1.00[a]
A1	1.00[a]		1.00[a]		1.00[a]
A2	1.00[a]		0.53	± 0.04	0.53(±0.04)
λ	435 (550) nm		435 (550) nm		435 & 550 nm
T1	18000 K[a]	18700 K[a]		18700K[a]	
T2	13500 K[a]		12934 K	±42 K	12808K(±100K
q	0.83[a]		0.702	± 0.002	0.788(±0.07)
Ω_1	3.776	± 0.013	3.611	± 0.004	3.841(±0.10)
Ω_2	3.990	± 0.022	3.482	± 0.003	3.701(±0.10)
r_1 pole	0.335		0.340		0.324
r_1 point	0.382		0.381		0.360
r_1 side	0.347		0.361		0.337
r_1 back	0.364		0.367		0.348
r_2 pole	0.282		0.296		0.299
r_2 point	0.310		0.339		0.341
r_2 side	0.289		0.318		0.313
r_2 back	0.302		0.324		0.326
σ	....		0.0067(0.0088)[b]		0.013(0.015)
d. pts.	....		2 x 335		2 x 335

a = fixed quantity
b = weighted [b = 1/2]

TABLE 2

Simplex solution of BBG B data. Only parameters subject to optimization are shown.

Parameter	Value
i	83?3
q	0.74
Ω_1	3.744
Ω_2	3.615
T_2	12883
A_2	0.51
σ	0.0119

TABLE 3

Simplex simultaneous solution of MP B, V data. Only parameters subject to optimization are shown.

Parameter	Value
i	83°3
q	0.75
Ω_1	3.753
Ω_2	3.623
T_2	12921
A_2	0.52
σ	0.0246

REFERENCES

Battistini, P., Bonifazi, A., and Guarnieri, A. 1972, Astrophys. Space Sci., 19, 385.

Eaton, J.A. 1975, Ap. J., 197, 379.

Hall, D.S., and Hardie, R.H. 1969, Publ. Astron. Soc. Pacific, 81, 754.

Hill, G., and Hutchings, J.B. 1973a, Astrophys. Space Sci., 20, 123.

Hill, G., and Hutchings, J.B. 1973b, Astron. and Astrophys., 23, 357.

Hill, G. 1979, Publ. D.A.O. 15, 322.

Iben, I. 1967, in Ann. Rev. Astron. Ap., 5, 571.

Kallrath, J., and Linnell, A.P. 1987, Ap. J., in press.

Lavrov, M.I. 1965, Bull. Engelhardt Obs., 38, 3.

Leung, K.-C., and Wilson, R.E. 1977, Ap. J., 211, 853.

Linnell, A.P. 1973, Astrophys. Space Sci., 22, 13.

_____. 1984, Ap. J. Suppl., 54, 17.

Mihalas, D. 1978, Stellar Atmospheres, 2nd ed., (San Francisco: Freema p. 51.

Murnikova, V.P., and Paramonova, O.P. 1980, Peremennye Zvedzdt, 21, 455.

Napier, W.M.D. 1971, Astrophys. Space Sci., 11, 375.

Popper, D.M. 1984, Astron. J., 89, 132.

Proctor, D.D., and Linnell, A.P. 1972, Ap. J. Suppl., 24, 449.

Rucinski, S. 1969, Acta Astron., 19, 245.

_____. 1970, Acta Astron., 20, 327.

Schmidt-Kaler, Th. 1982, in Landolt-Börnstein: Numerical Data and Functional Relationships in Science and Technology,(vol. 2), (Berlin: Springer-Verlag).

Söderhjelm, S. 1974, Astron. and Astrophys., 34, 59.

_____. 1978, ibid., 66, 161.

Tassoul, J.-L. and Tassoul, M. 1982a, Ap. J. Suppl., 49, 317.

_____. 1982b, Ap. J., 261, 265.

_____. 1982c, ibid., 261, 273.

_____. 1983, ibid., 264, 298.

Underhill, A.B. and Fahey, R.P. 1984, Ap. J., 280, 712.

Vaz, L.P.R. 1985, Astrophys. Space Sci., 113, 329.

Vaz, L.P.R., and Nordlund, A. 1985, Astron. Astrophys., 147, 281.

Wilson, R.E., and Devinney, E.J. 1971, Ap. J., 166, 605.

Wilson, R.E., DeLuccia, M.R., Johnston, K., and Mango, S.A. 1972, Ap. J., 177, 191.

Wilson, R.E., and Devinney, E.J. 1972, Ap. J., 171, 413.

Wilson, R.E. 1979, Ap. J., 234, 1054.

Figure Captions

Fig. 1- MR Cyg V light curve fit and residuals, simultaneous V and B solution with SYNPGM and the simplex algorithm. System parameters are in Table 1. The residuals ordinate has a scale factor of 10^2.

Fig. 2- B residuals, same solution as Figure 1. The ordinate has a scale factor of 10^2.

Fig. 3- U residuals, geometric parameters from the V, B solution of Figures 1 and 2. The ordinate has a scale factor of 10^2.

Fig. 4- Comparison of B observations with theoretical light curve with bolometric albedo A2 = 1.0. Other parameters in Table 1.

Fig. 5- Orbital phase variation of B3 component with eclipse effects removed. The ordinate gives the correct fractional contribution to system light.

Fig. 6- Orbital phase variation of secondary component with eclipse effects removed, and with a bolometric albedo A2 = 1.0. The ordinate gives the correct fractional contribution to system light. The single cycle variation, as contrasted with Figure 5, shows that reflection effect dominates this light variation.

Fig. 7- Fit to the B observations with bolometric albedo of the secondary component A2 = 0.5. Other parameters in Table 1.

Fig. 8- Orbital phase variation of secondary component but with bolometric albedo A2 = 0.5.

Fig. 9- V and B light curve solution locations for the secondary component, assuming the primary component is a B3 main sequence object.

Fig. 10- Mass vs. spectral class diagram showing the main sequence, the primary at adopted spectral class B3, and limiting locations for

the secondary based on a photometric q. The marked B7(+) location is based on the derived spectral class from Figure 9. See text.

Fig. 11- A geometric model of MR Cyg based on a simultaneous solution of V, B data and an assumed main sequence mass for the primary component.

Fig. 1

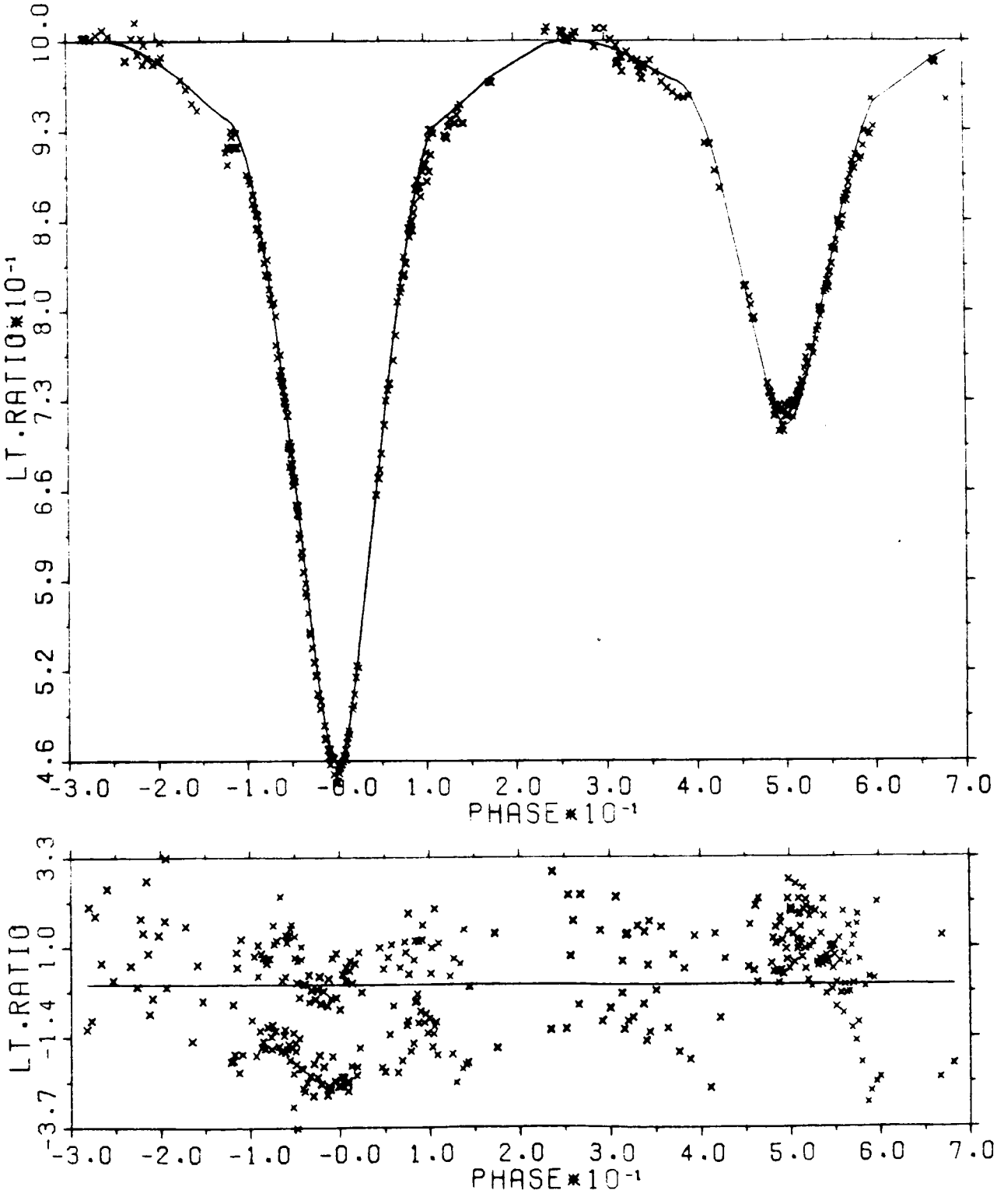

Fig. 2

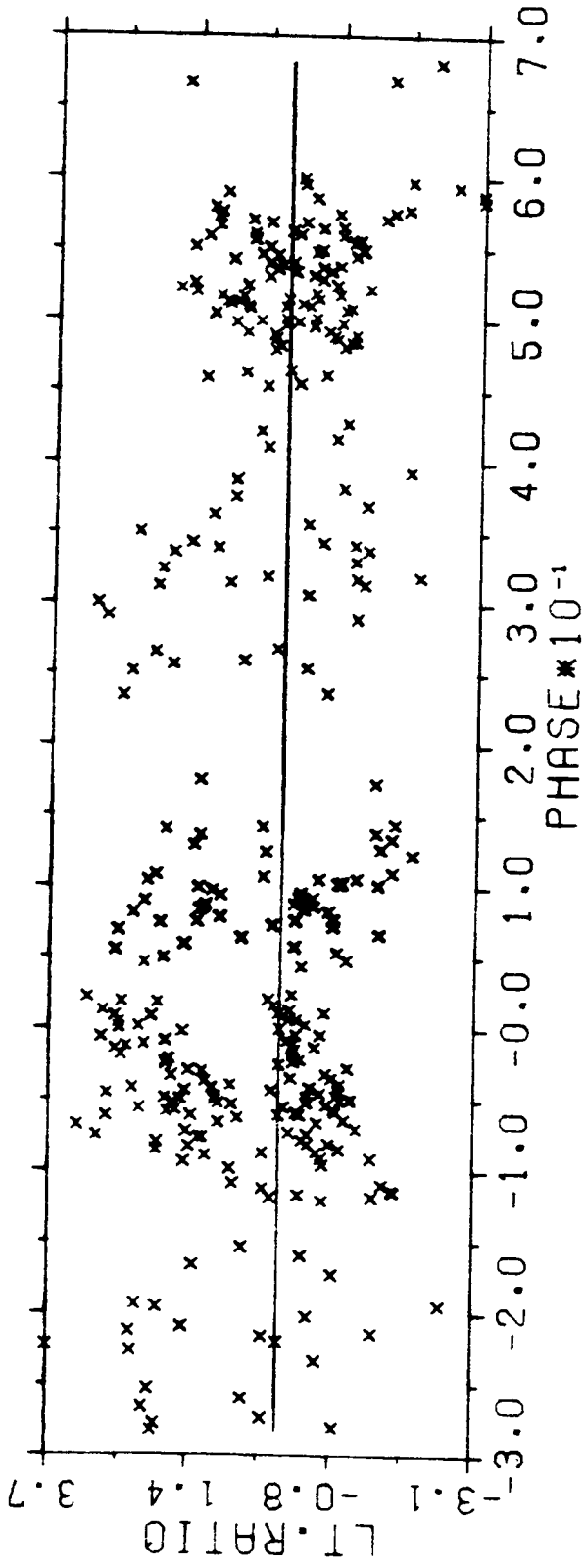

Fig. 3

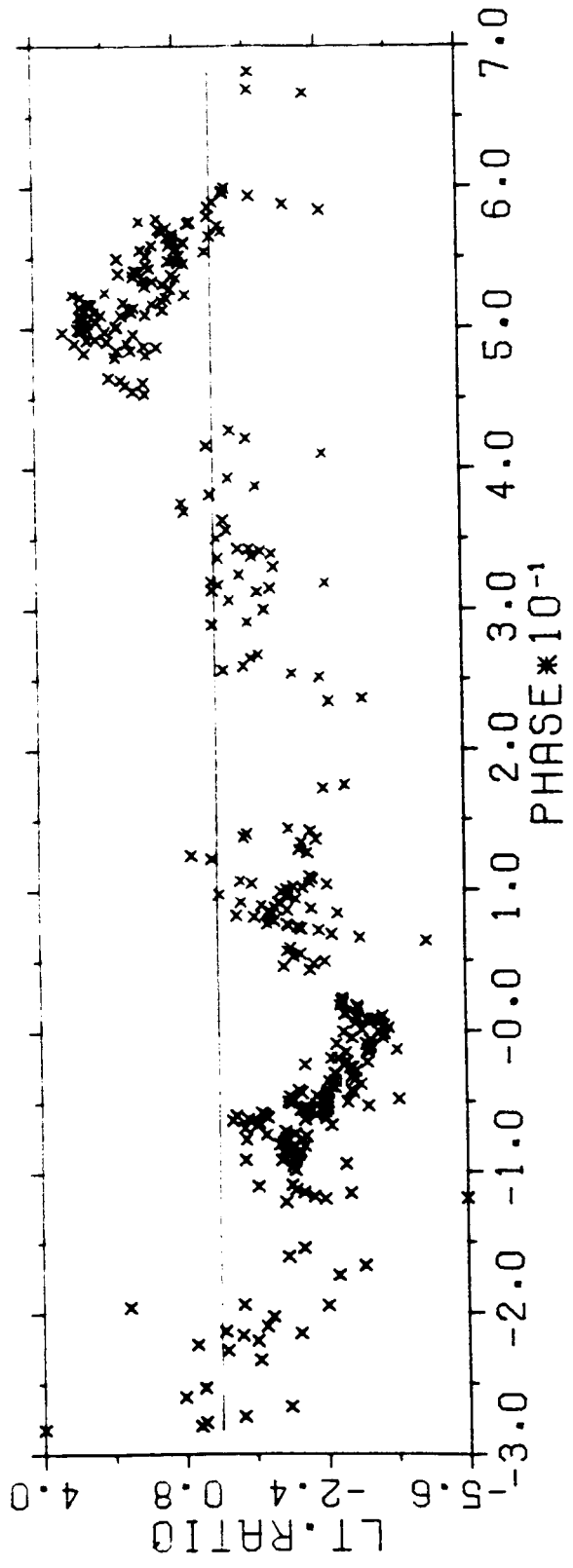

Fig. 4

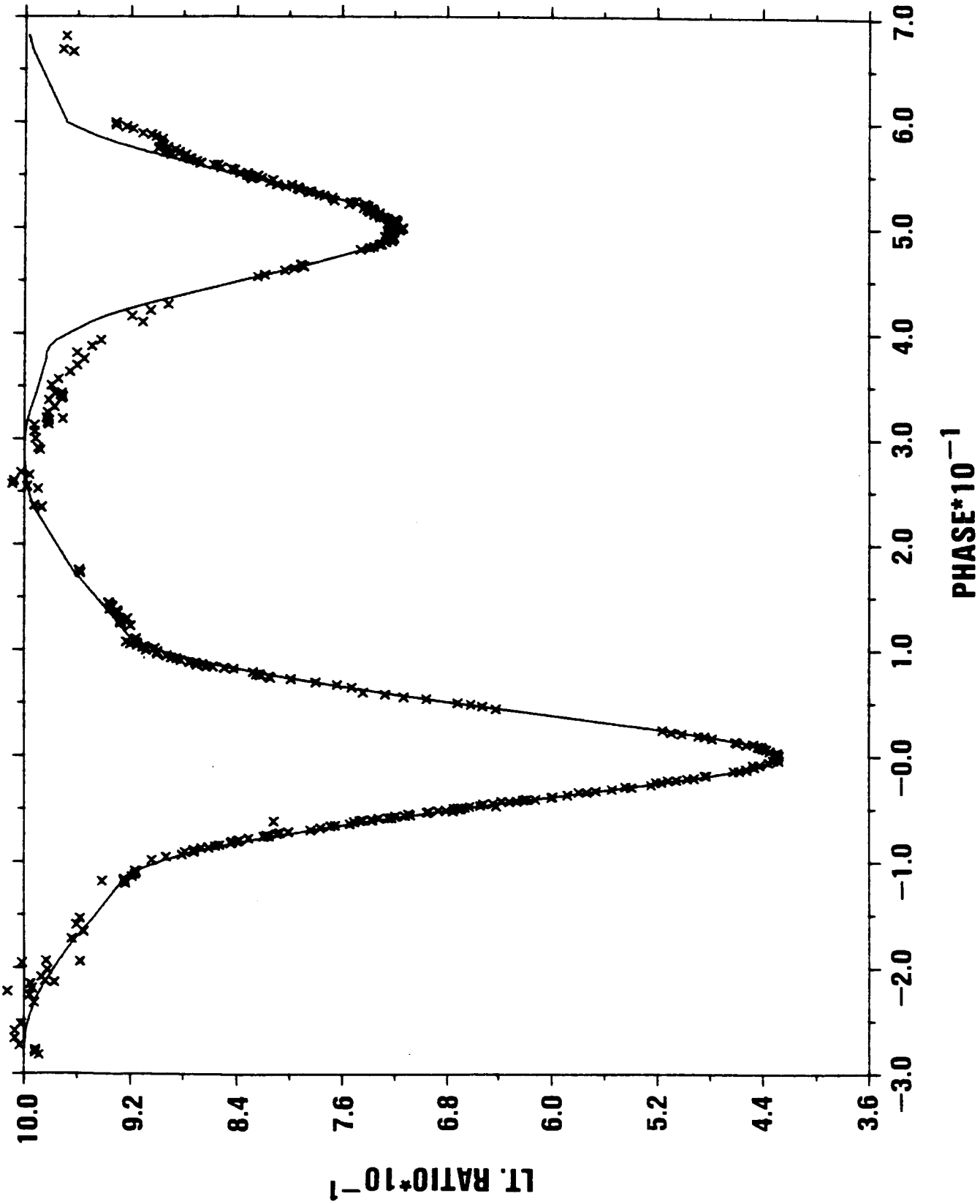
LT. RATIO*10⁻¹
10.0
9.2
8.4
7.6
6.8
6.0
5.2
4.4
3.6
−3.0
−2.0
−1.0
−0.0
1.0
2.0
3.0
4.0
5.0
6.0
7.0
PHASE*10⁻¹

Fig. 5

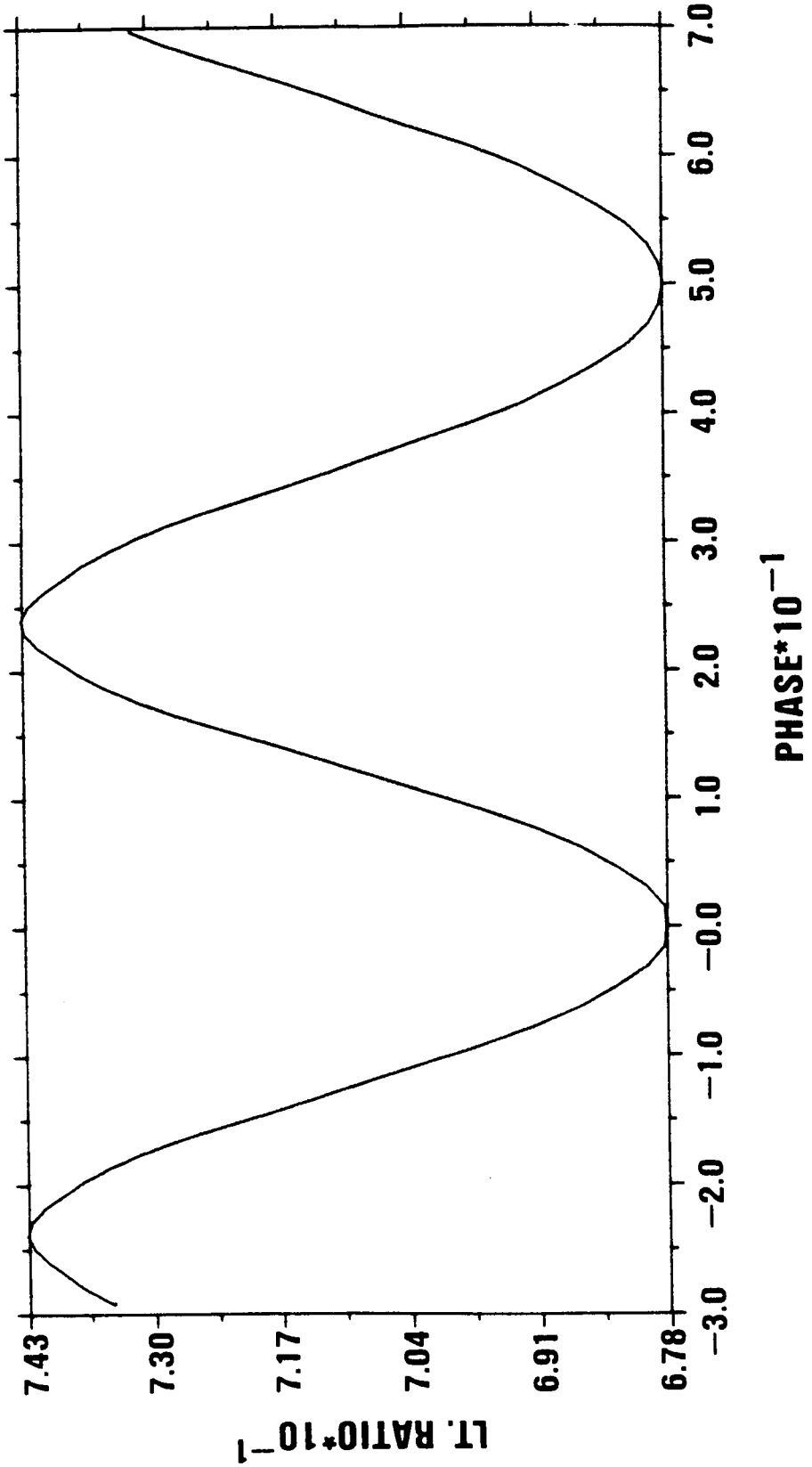
7.43
7.30
7.17
7.04
6.91
6.78
LT. RATIO*10⁻¹
-3.0
-2.0
-1.0
-0.0
1.0
2.0
3.0
4.0
5.0
6.0
7.0
PHASE*10⁻¹

Fig. 6

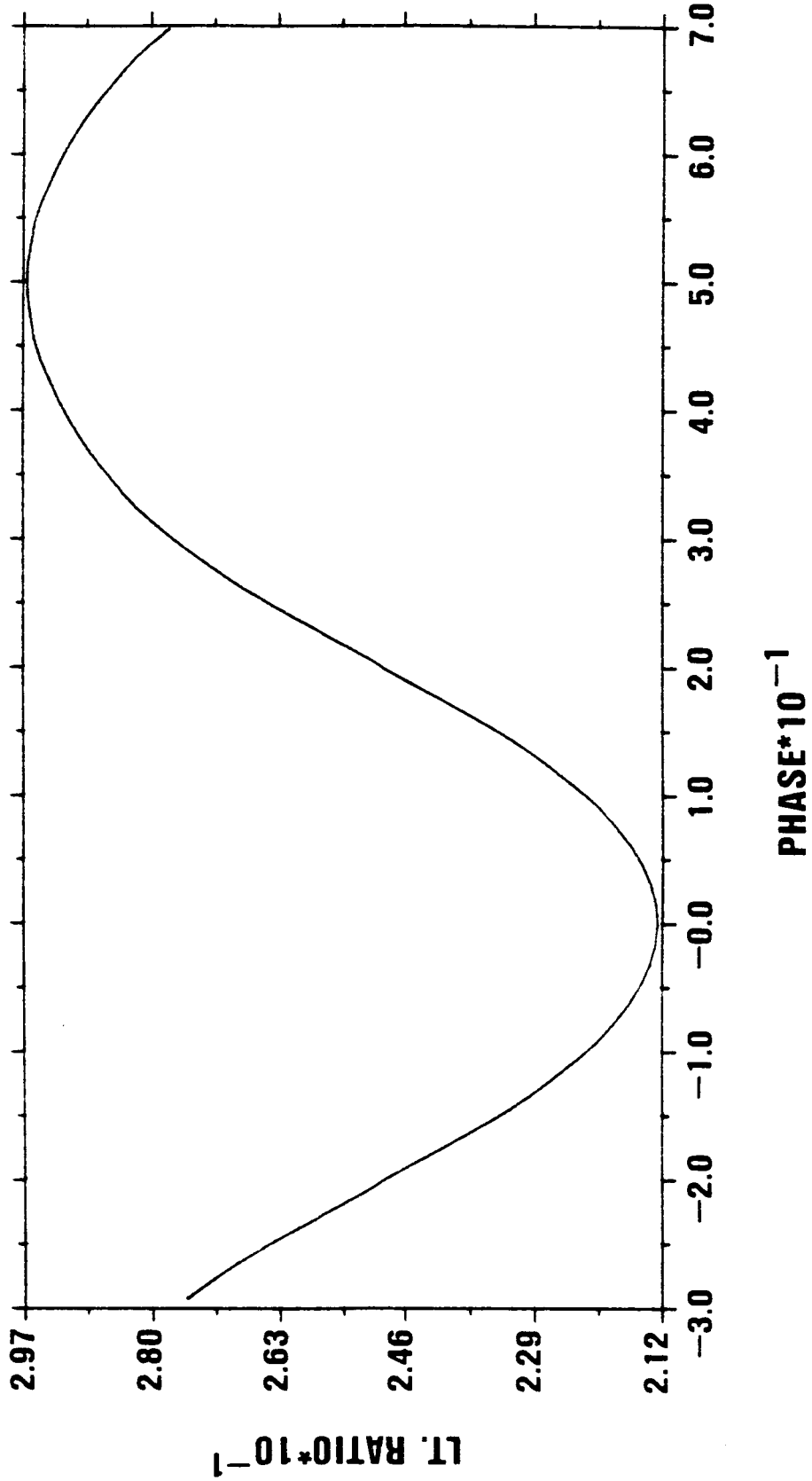
LT. RATIO*10⁻¹
2.97
2.80
2.63
2.46
2.29
2.12
−3.0
−2.0
−1.0
−0.0
1.0
2.0
3.0
4.0
5.0
6.0
7.0
PHASE*10⁻¹

Fig. 7

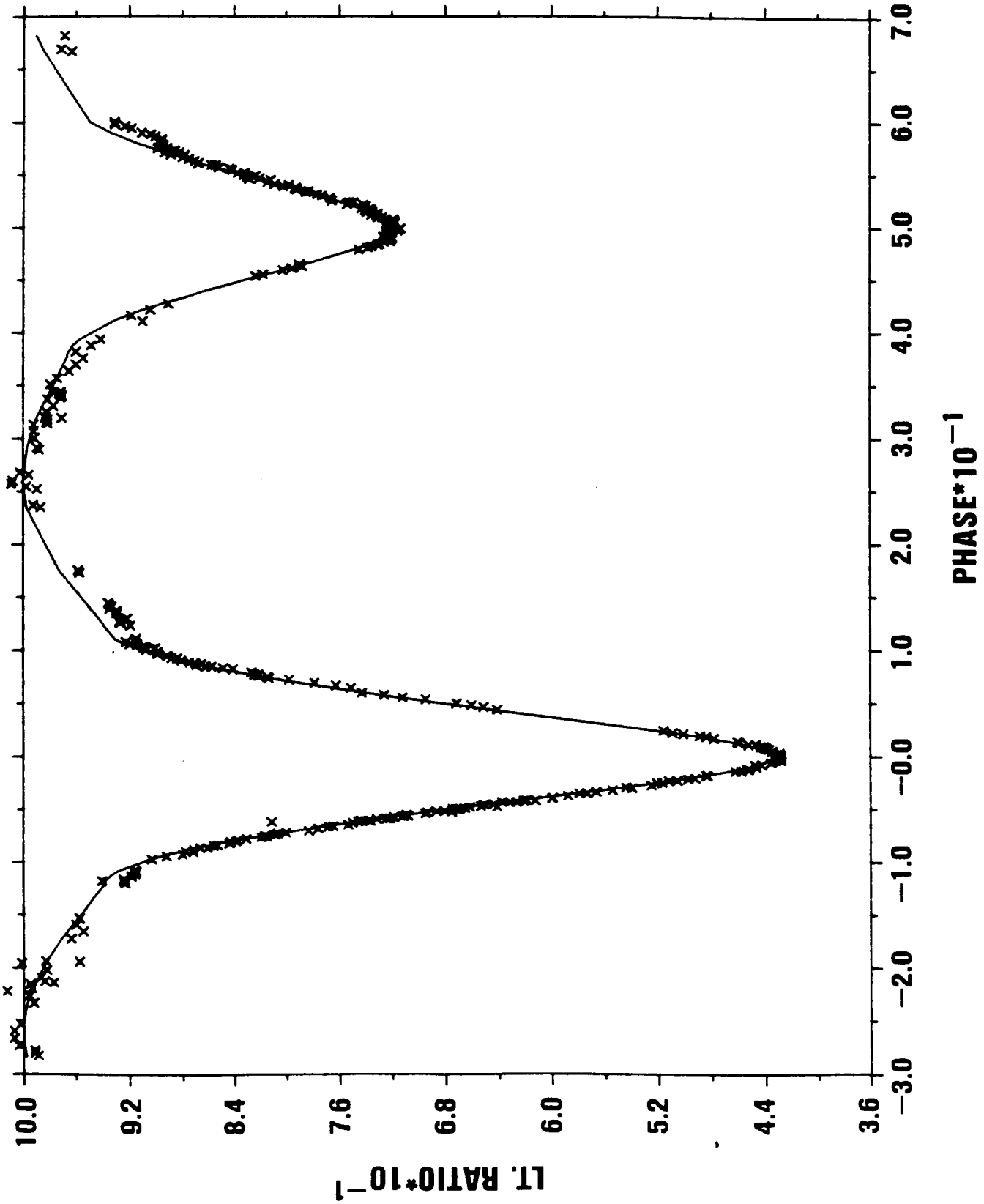
LT. RATIO*10⁻¹
10.0
9.2
8.4
7.6
6.8
6.0
5.2
4.4
3.6
PHASE*10⁻¹
-3.0
-2.0
-1.0
-0.0
1.0
2.0
3.0
4.0
5.0
6.0
7.0

Fig. 8

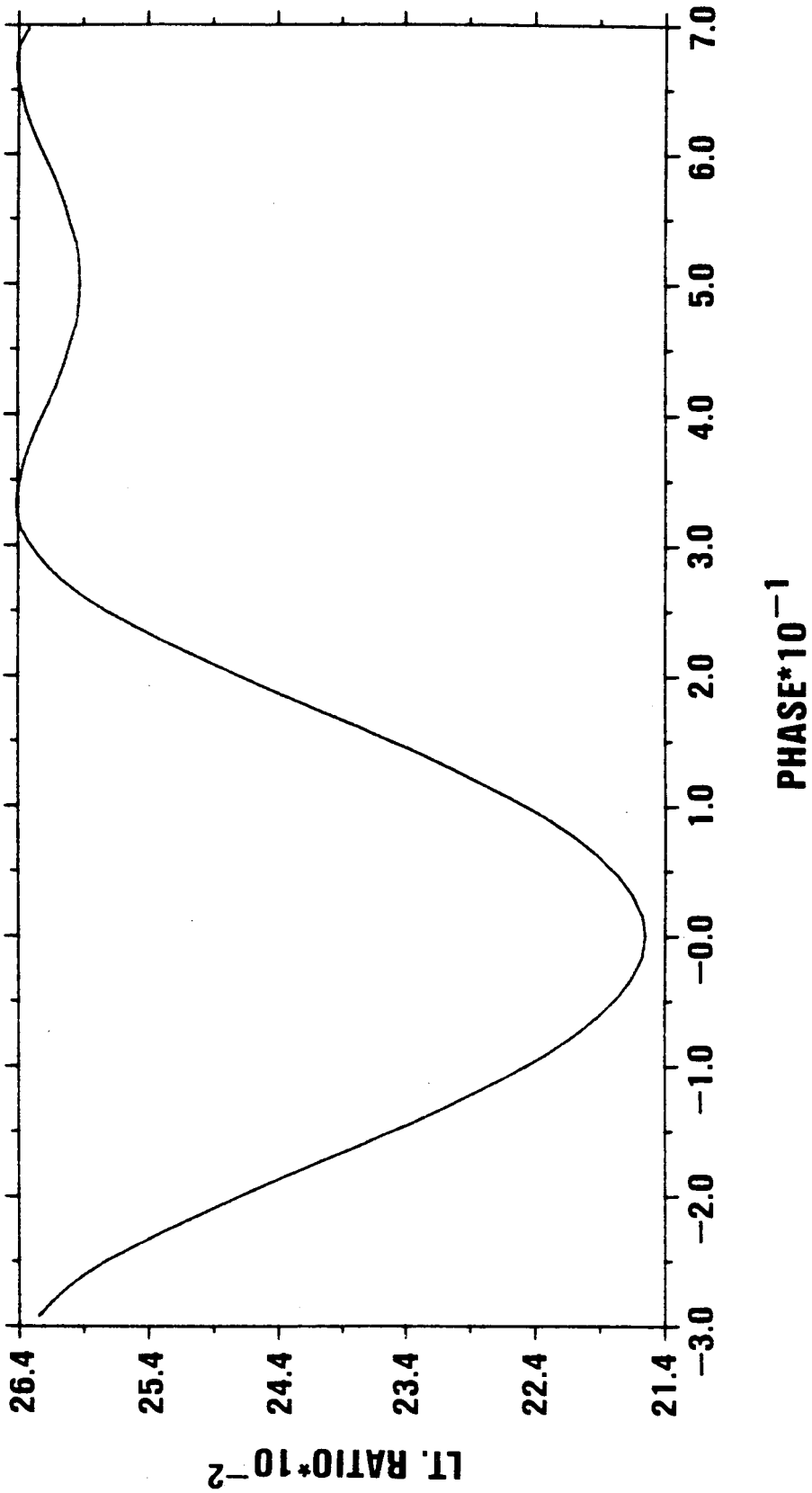
LT. RATIO*10⁻²
26.4
25.4
24.4
23.4
22.4
21.4
−3.0
−2.0
−1.0
−0.0
1.0
2.0
3.0
4.0
5.0
6.0
7.0
PHASE*10⁻¹

Fig. 9

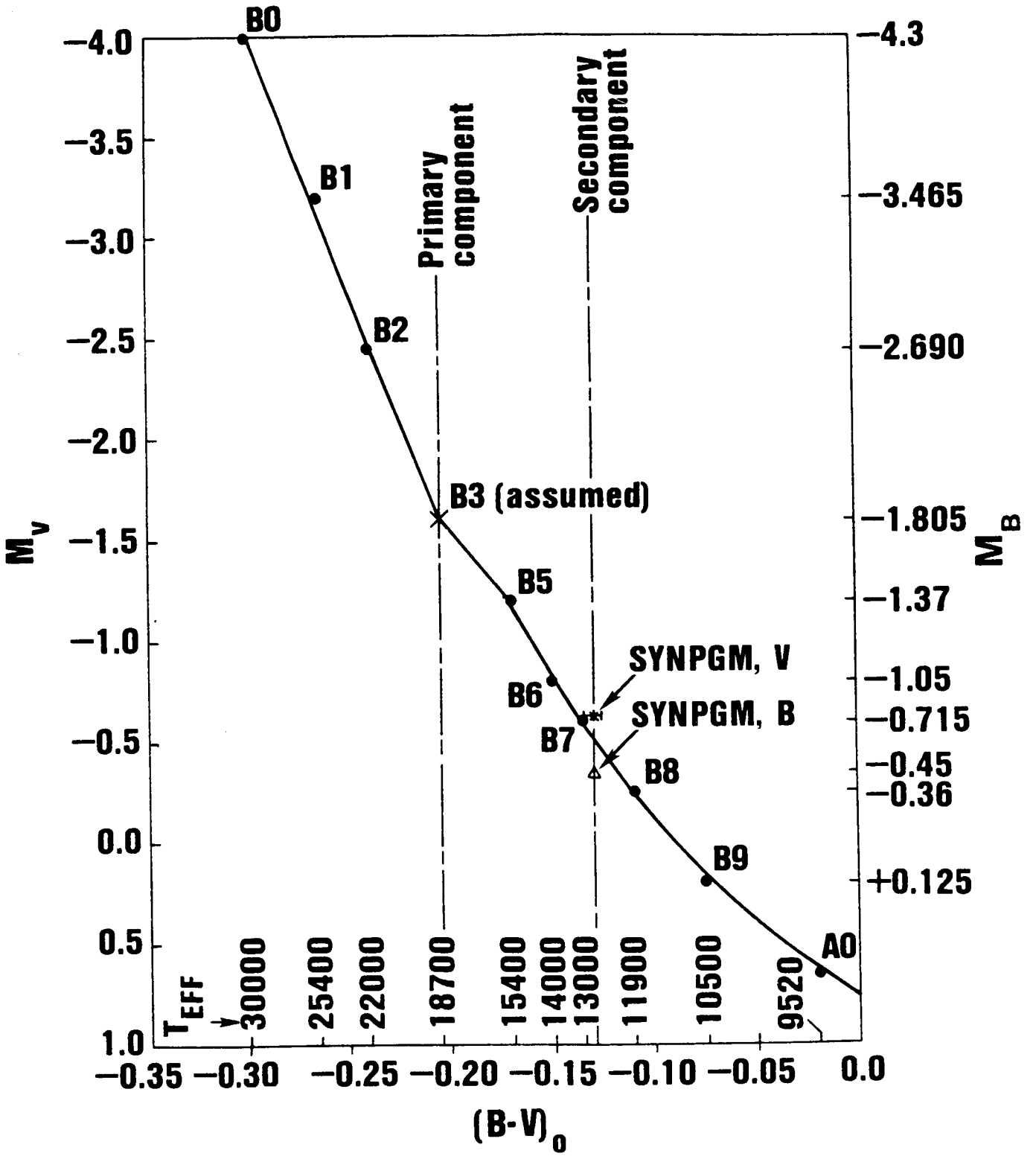
B0
B1
B2
B3 (assumed)
B5
B6
B7
B8
B9
A0
Primary component
Secondary component
SYNPGM, V
SYNPGM, B
M_V
M_B
−4.0
−3.5
−3.0
−2.5
−2.0
−1.5
−1.0
−0.5
0.0
0.5
1.0
−4.3
−3.465
−2.690
−1.805
−1.37
−1.05
−0.715
−0.45
−0.36
+0.125
T_{EFF}
30000
25400
22000
18700
15400
14000
13000
11900
10500
9520
−0.35 −0.30 −0.25 −0.20 −0.15 −0.10 −0.05 0.0
$(B-V)_0$

Fig. 10

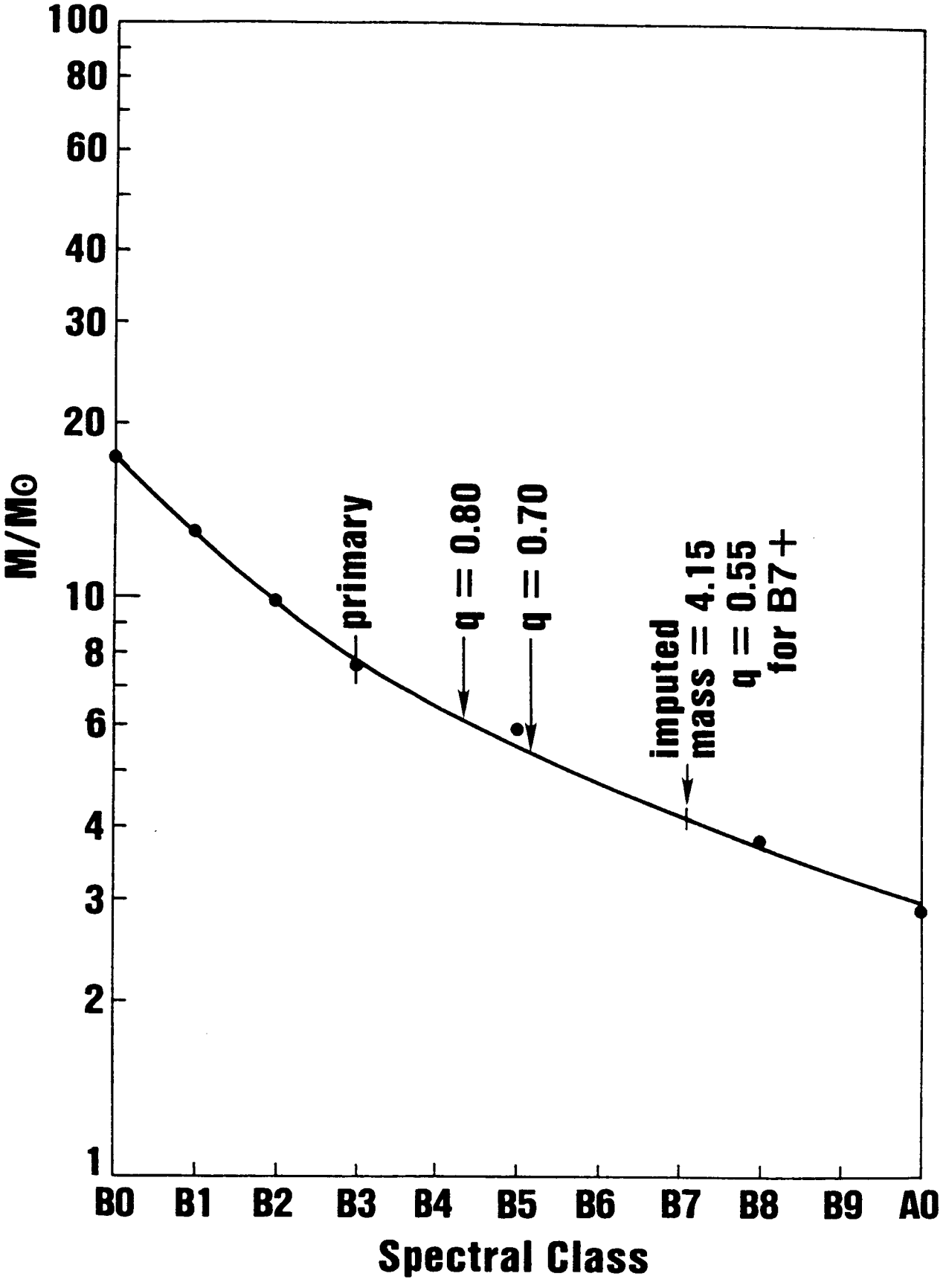
100
80
60
40
30
20
10
8
6
4
3
2
1
M/M⊙
primary
q = 0.80
q = 0.70
imputed
mass = 4.15
q = 0.55
for B7+
B0
B1
B2
B3
B4
B5
B6
B7
B8
B9
A0
Spectral Class

Fig. 11

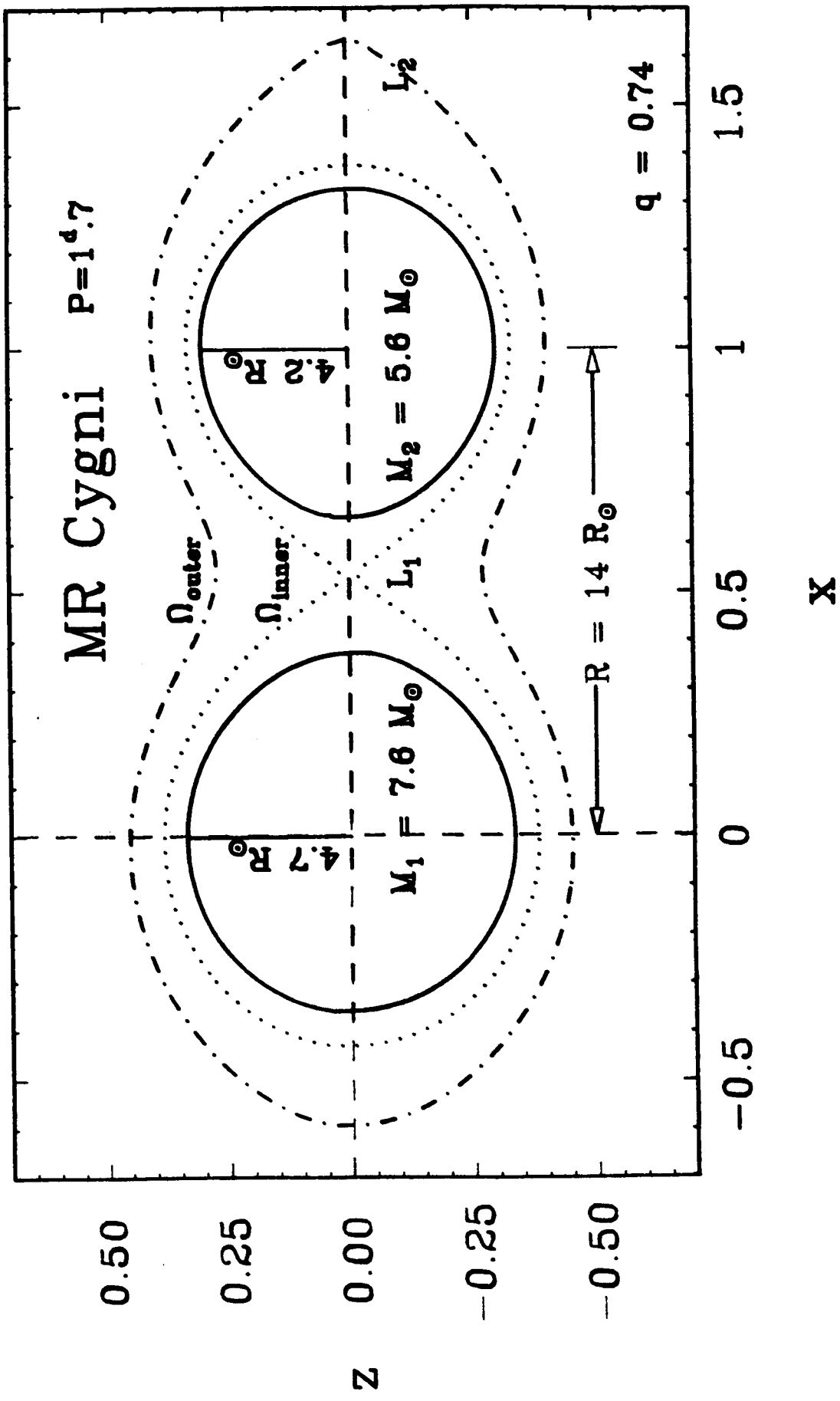
MR Cygni P=1d.7
q = 0.74
L2
L1
Ωouter
Ωinner
M2 = 5.8 M⊙
M1 = 7.8 M⊙
4.2 R⊙
4.7 R⊙
R = 14 R⊙
1.5
1
0.5
0
−0.5
X
0.50
0.25
0.00
−0.25
−0.50
Z

Albert P. Linnell

Department of Physics and Astronomy

Michigan State University

East Lansing, MI 48824-1116

Josef Kallrath

Sternwarte der Universitat Bonn

Auf dem Hugel 71

D-5300 Bonn 1

Federal Republic of Germany